

# Thermal kinetics of montmorillonite nanoclay/maleic anhydride-modified polypropylene nanocomposites

Henry Kuo Feng Cheng · Nanda Gopal Sahoo ·  
Xuehong Lu · Lin Li

Received: 7 November 2010 / Accepted: 17 March 2011 / Published online: 30 March 2011  
© Akadémiai Kiadó, Budapest, Hungary 2011

**Abstract** Thermal kinetics of montmorillonite nanoclay (MMT)/maleic anhydride-modified polypropylene (MAH-PP) composites (PPCNs) is reported here in terms of thermal stability, decomposition, and crystallization kinetics. The effects of MMT nanoclay on the thermal stability of PP in MMT/MAH-PP composites have been examined at different heating rates by means of thermogravimetric (TG) analysis. Based on the TG results, the Ozawa method was applied to determine the activation energies of decomposition for MMT/MAH-PP composites and the results were then verified by the Kissinger method. It was found that the thermal stability of PP was significantly improved in the presence of MMT nanoclay. Differential scanning calorimetry (DSC) was used to study the melting and crystallization behaviors of MMT/MAH-PP composites under various thermal conditions. Using the data from DSC, the Kissinger method was applied to estimate the activation energies of PPCNs which were required during their non-isothermal crystallization. The activation energies of crystallization showed that MMT nanoclay served as a nucleating agent in the non-isothermal crystallization of PP in the PPCNs and as a result, the crystallinity of PP was greatly enhanced. Therefore, the presence of MMT nanoclay in MMT/MAH-PP composites effectively modified the thermal kinetics of PP.

**Keywords** Polymer nanocomposite · Crystallization · Thermal degradation · Activation energy · Clay composite

## Introduction

In the current century, polymer nanocomposites have pulled a great attraction from material scientists and researchers due to their potentially novel properties. Various types of nanofillers such as nanoclay, carbon nanotubes (CNT), calcium carbonate ( $\text{CaCO}_3$ ), silica ( $\text{SiO}_2$ ), titanium oxide ( $\text{TiO}_2$ ), and zinc oxide ( $\text{ZnO}$ ), have been added into a polymer matrix for various reasons such as, property improvement and cost reduction [1].

Polypropylene (PP) is one of the most commonly used thermoplastic polymers due to its well-known physical and mechanical properties as well as the ease of processing at a relatively low cost. In the recent years, polypropylene nanocomposites have received a great attention because of their high potentials for improvement of physical properties over neat PP and its conventional composites. There is a number of research papers on the polypropylene nanocomposites filled with different types of fillers such as carbon nanotubes (CNTs) [2–4], nanoclay [5–7], etc. Among several types of fillers, nanoclay is of a high potential due to its lower cost over its counter parts and its effective enhancement on the overall properties of the composites. The preparation and properties of clay/polypropylene nanocomposites (PPCNs) have been extensively reported and discussed in the literature [6–10]. It has been known that the properties of PPCNs are greatly affected by the intercalation and exfoliation of nanoclay in a PP matrix [7, 10].

However, the detailed studies on the effects of nanoclay on the thermal kinetics of PP in the PPCNs have not been

---

H. K. F. Cheng · N. G. Sahoo · L. Li (✉)  
School of Mechanical and Aerospace Engineering,  
Nanyang Technological University, 50 Nanyang Avenue,  
639798 Singapore city, Singapore  
e-mail: mlli@ntu.edu.sg

X. Lu  
School of Material Science and Engineering,  
Nanyang Technological University, 50 Nanyang Avenue,  
639798 Singapore city, Singapore

found in the literature. Therefore, in this work, the effects of nanoclay on the thermal decomposition and stability, crystallization and melting behaviors of PP filled with various contents of nanoclay and under different thermal conditions have been systematically examined. The MMT nanoclay content in the composites was varied from 0 to 6% mass in order to study the influence of nanoclay content on the thermal properties. Particularly, we have investigated the mechanism for how nanoclay could modify the degradation kinetics and non-isothermal crystallization kinetics of PP.

## Experimental

Maleic anhydride-modified polypropylene (MAH-PP) and MAH-PP/montmorillonite (MMT) nanocomposite with a nanoclay content of 6% mass, which were supplied in pellet form, by Nanocor Inc. Transmission electron microscopic images of the nanocomposite provided by Nanocor confirmed a large extent of exfoliation and preferred orientation of nanoclay layers in the nanocomposite [11]. In order to study the influence of nanoclay content on the thermal kinetics, the nanocomposite with 6% mass nanoclay was dry-mixed with MAH-PP to achieve nanoclay contents of 2 and 4% mass, respectively. The mixtures were then extruded with a Brabender twin-screw extruder at a screw speed of 30 rpm. The temperature at the nozzle was set at 200 °C. The composite samples were denoted with PPCN0, PPCN2, PPCN4, and PPCN6 for the MMT nanoclay contents of 0, 2, 4, and 6% mass, respectively. All the samples were dried in a vacuum oven at 40 °C for 24 h and then kept in a dry box before use.

Thermogravimetric (TG) Analysis is usually used to measure the amount and rate of change in the mass of a material as a function of temperature or time in a controlled atmosphere. To study the degradation behavior and kinetics of PP in the composites, the samples were heated from room temperature to 600 °C using a TG analyzer (TA Instruments, TGA-2950), and the mass loss of each sample was measured as a function of temperature at a given heating rate. Four heating rates were employed (2.5, 5, 10, and 20 °C min<sup>-1</sup>) for the studies of thermal degradation kinetics. Nitrogen gas was used as the purge gas in this study.

A differential scanning calorimeter (DSC, TA Instruments DSC2920) was used to study the non-isothermal melting and crystallization kinetics of PP in PPCNs. The samples were heated and cooled at four different rates of 2.5, 5, 10, and 20 °C min<sup>-1</sup> under a nitrogen environment. The experiments were carried out with two temperature scans. The first scan was used to eliminate any possible thermal and mechanical history of a sample and the second

one was for the characteristic properties of the sample [12, 13]. In the first scan, the sample was heated from -50 to 250 °C at the respective heating rate, and held at 250 °C for 5 min, and then cooled at the same rate back to -50 °C. Then, this procedure was repeated as the second scan. As the second scan was related to the characteristic properties of the sample, the DSC curves shown in this work were obtained from the second scan.

## Results and discussion

### Thermal stabilities of MMT clay/MAH-PP nanocomposites

TG provides information regarding the mass loss of a sample due to thermal degradation in two different forms: mass loss as a function of either temperature or time, and the derivative of mass loss as a function of temperature or time. The former is a direct indication of mass loss as a function of temperature or time while the latter indicates the rate of mass loss as a function of temperature or time [13–16]. The TG measurements were carried out for the four composite samples (i.e. PPCN0, PPCN2, PPCN4, and PPCN6) at four heating rates. Figure 1a illustrates the TG curves for the four composite samples studied at a heating rate of 10 °C min<sup>-1</sup>. The curves before 300 °C are not shown in this figure as there was no considerable mass loss for each composite detected below this temperature.

The thermal stability of PP in the pure form and in the nanoclay composites can be observed from the TG curves in Fig. 1a. All four samples showed mass losses less than 5% up to 350 °C, and then they started to decompose more with increasing temperature. The pure PP degraded with a slower rate with temperature than the others and its complete decomposition (i.e. 100% mass loss) was achieved at a temperature near 450 °C. On the other hand, three composites showed the similar pattern of mass loss with a faster rate than the pure PP. In this work, the criteria for the thermal stability were taken as the temperatures at 5% mass loss occurred in the samples at the heating rate of 10 °C min<sup>-1</sup>. The 5% decompositions for neat PP, PPCN2, PPCN4, and PPCN6 occurred at 385, 408, 414, and 415 °C, respectively. Therefore, the 5% decomposition temperatures increased with increase in the MMT content in the composites. On the other hand, the MMT/PP composites showed the delayed decomposition compared to the pure PP incorporated with MMT nanoclay. For example, the 5% decomposition of PPCN6 occurred at 415 °C which is 30 °C enhancement in the thermal stability compared to the pure PP. Therefore, the thermal stability of PP was significantly improved in the presence of MMT clay. From the temperature derivative curves in Fig. 1b, the maximum

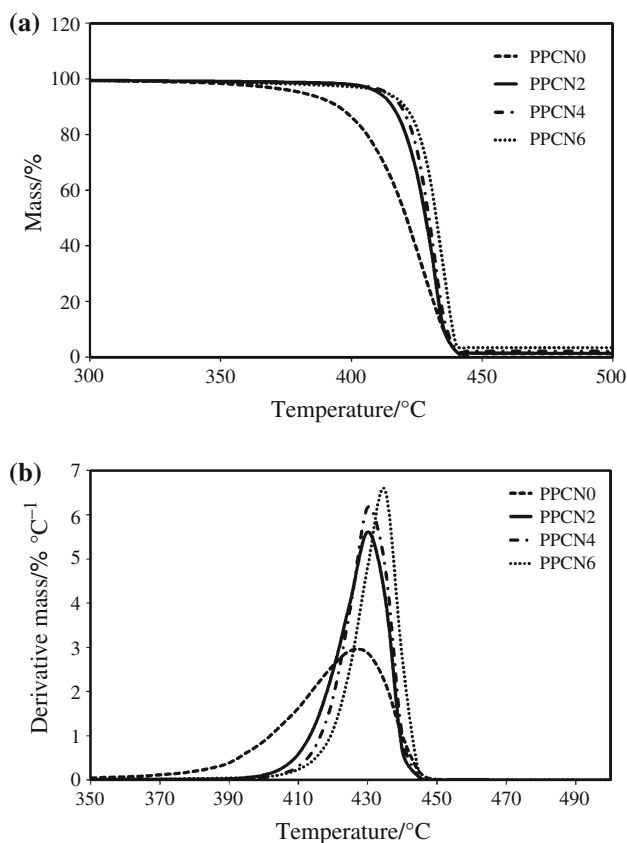


**Fig. 1** **a** TG curves for PPCN composites at a heating rate of  $10\text{ }^{\circ}\text{C min}^{-1}$  and **b** Temperature derivatives of the TG curves in (a)

degradation rate occurred at 425, 431, and 436  $^{\circ}\text{C}$  for PPCN2, PPCN4, and PPCN6, respectively, which are all higher than that of the pure PP (420  $^{\circ}\text{C}$ ). At other heating rates (2.5, 5, and 20  $^{\circ}\text{C min}^{-1}$ ), the similar results were obtained. Therefore, it can be concluded that, incorporated with MMT nanoclay, PP showed better thermal stability.

We propose several reasons for why the PPCN nanocomposites exhibited better thermal stabilities than the pure PP. First, it is due to the better thermal conductivity of the nanoclay composites, which results in a better heat transfer to PP through the bulk sample. Several literatures [2, 4, 17–19] reported that the thermal stability of a polymer is greatly enhanced in the presence of thermally conductive fillers. The second one is concerned to the interactions between the components in the composites. Due to the maleic anhydride modification of PP, the interaction between MMT and MAH-PP has been greatly enhanced. Because of this stronger adhesion between MMT and MAH-PP, the composites show the higher thermal stabilities. The last one is considered to be related with the packing density of a composite sample. Due to the strong interaction between MMT nanoclay and MAH-PP, the nanocomposites would have higher packing densities than that of pure PP. This also is in agreement with our previous

publication [20]. In that work, we reported that if there is an interaction between the components of a nanocomposite, the bulk density of the composite could be remarkably increased. Therefore, a sample with a higher packing density would have a slower decomposition pattern, as often observed in TG measurements.

Finally, at the end temperature (600  $^{\circ}\text{C}$ ) of TG measurements, the pure PP produced no residue while PPCN2, PPCN4, and PPCN6 had about 2, 4, and 6% mass residues, respectively. Therefore, it was proved that the sample compositions were as correct as they had been formulated. The results also indicated that the nanoclay filler was thermally stable and it did not degrade up to 600  $^{\circ}\text{C}$ .

#### Thermal decomposition kinetics of MMT clay/MAH-PP nanocomposites

Since heating rate applied governs the reaction time available at an observing temperature, the degradation kinetics will be affected by the heating rate applied. In general, it is known that the lower the heating rate, the longer time will be available for the reaction to take place. In order to study the decomposition kinetics using the Ozawa method [21–24], one has to use two or more heating rates. Therefore in this work, all the samples were tested at four heating rates: 2.5, 5, 10, and 20  $^{\circ}\text{C min}^{-1}$ .

A general pattern of thermogravimetric (TG) curves at a given mass loss is that at a lower heating rate (e.g. 2.5  $^{\circ}\text{C min}^{-1}$ ) the sample decomposes at lower temperatures, while at a higher rate (e.g. 20  $^{\circ}\text{C min}^{-1}$ ), it decomposes at higher temperatures. Thus, thermal stability is a function of heating rate and it is directly proportional to the heating rate. Based on this observation, it is possible to estimate the activation energy of a sample which is required for thermal degradation. The Ozawa method is often used to determine the activation energy of degradation under the following set of equations and assumptions [21–25].

In thermogravimetric (TG) analysis, the rate of degradation reaction ( $\alpha$ ) can be defined as the ratio of actual mass loss to the total mass loss corresponding to the degradation process.

$$\alpha = \frac{m_0 - m}{m_0 - m_f}, \quad (1)$$

where  $m_0$ ,  $m$ , and  $m_f$  are the initial, actual, and final masses of a test sample, respectively.

The rate of degradation ( $d\alpha/dt$ ) is a function of temperature and mass of the sample:

$$\frac{d\alpha}{dt} = kf(\alpha). \quad (2)$$

Here,  $k$  is the rate constant and a function of temperature.  $f(\alpha)$  is the rate of conversion and

**Fig. 2** Plots of  $\ln \beta$  against  $1000/T$  at various mass losses for the Ozawa method.  $\beta$  is the heating rate and  $T$  is the absolute temperature. **a**, **b**, **c**, and **d** are for PPCN0, PPCN2, PPCN4, and PPCN6, respectively

proportional to the concentration of the reactant. The  $f(\alpha)$  can be written as:

$$f(\alpha) = (1 - \alpha)^n \quad (3)$$

where,  $n$  is a power index.

The temperature dependence of the rate constant  $k$  is often described by the Arrhenius equation in which  $k$  is linked to the apparent activation energy,  $E_a$ :

$$k = A \exp\left(-\frac{E_a}{RT}\right), \quad (4)$$

where  $A$  is the pre-exponential factor,  $R$  the gas constant, and  $T$  the absolute temperature. The combination of Eqs. 2, 3, and 4 yields the following equation:

$$\frac{d\alpha}{dt} = A \exp\left(-\frac{E_a}{RT}\right) (1 - \alpha)^n. \quad (5)$$

By introducing the heating rate,  $\beta = (dT/dt)$ , Eq. 5 becomes

$$\frac{d\alpha}{(1 - \alpha)^n} = \frac{A}{\beta} \exp\left(-\frac{E_a}{RT}\right) dT. \quad (6)$$

Thus, Eq. 6 is the basic relation to determine kinetic parameters on the basis of TG data. Through the further mathematic treatments including the Doyle approximation used in the Ozawa method, the following equation is derived:

$$\ln \beta = C - 1.052 \frac{E_a}{RT}, \quad (7)$$

where  $C$  is a constant at a given  $\alpha$ . Equation 7 is the expression of the Ozawa method. Thus, at a given heating rate ( $\beta$ ) and a particular mass loss ( $\alpha$ ), the corresponding temperature ( $T$ ) can be found. At a given mass loss ( $\alpha$ ) by varying heating rate ( $\beta$ ), the corresponding temperature ( $T$ ) is a function of  $\beta$ . Hence, if a plot of  $\ln \beta$  versus  $1/T$  is linear, the activation energy ( $E_a$ ) can be calculated from the slope of  $1.052E_a/R$ .

At all four heating rates (2.5, 5, 10, and 20 °C min<sup>-1</sup>) and different percent mass losses (i.e. 5–50%), all corresponding temperatures were found. According to Eq. 7, in order to obtain  $E_a$ ,  $\ln \beta$  was plotted against  $1000/T$  in Fig. 2 for all selected mass losses. In Fig. 2, each curve shows a constant mass loss percentage. Since the percent mass loss increases with degradation temperature, in each figure, a curve at the right side (i.e. lower temperature) has a lower mass loss percentage than that at the left side (higher temperature) along the axis of  $1000/T$ .

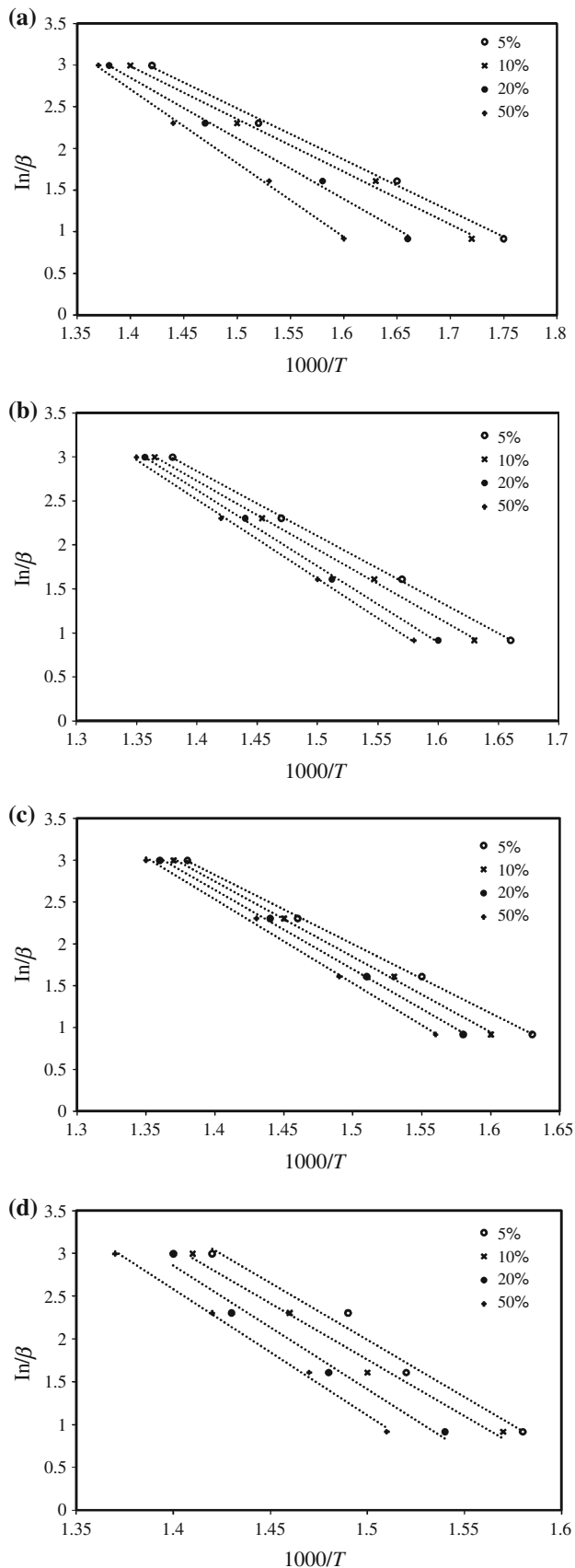


**Table 1** Average activation energies,  $E_a$ , of degradation for PPCNs, obtained using the Ozawa method

Sample code	PPCN0	PPCN2	PPCN4	PPCN6
Average activation energy/kJ mol <sup>-1</sup>	122.56	141.54	164.15	220.94

As theoretically described by Eq. 7, each curve in Fig. 2 has to be a straight line with a negative slope and all curves for each sample should be parallel with each other in order to give a constant activation energy ( $E_a$ ) if the sample's degradation kinetics obeys Eq. 7. As shown in Fig. 2, all curves are of negative slopes, indicating the possibility of using Eq. 7 to determine  $E_a$ . It is interesting to observe that the data points can be approximately fitted to the corresponding straight lines and they are nearly parallel for each composite. From the slopes,  $E_a$  could be calculated and averaged and then the results are shown in Table 1.

Moreover, the activation energies of degradation for PPCNs can also be studied by using the Kissinger method [21, 22]. In the case of the Kissinger method, the activation energy is calculated from the  $T_{max}$ , the temperature at which the maximum degradation occurs at different heating rates. The maximum rate occurs when  $dx/dt = 0$ , which is where the peak temperature of time derivative of a TG curve (i.e. similar to that of its temperature derivative). Thus, differentiating equation 6 with respect to time and equating the resulting expression to zero leads to the following equation:

$$\left(\frac{d^2\alpha}{dT^2}\right)_{max} = \left(\frac{d\alpha}{dT}\right)_{max} \times \left[ \frac{E_a}{RT_{max}^2} - \frac{nA}{\beta} \exp\left(-\frac{E_a}{RT_{max}}\right) (1 - \alpha)_{max}^{n-1} \right]. \quad (8)$$

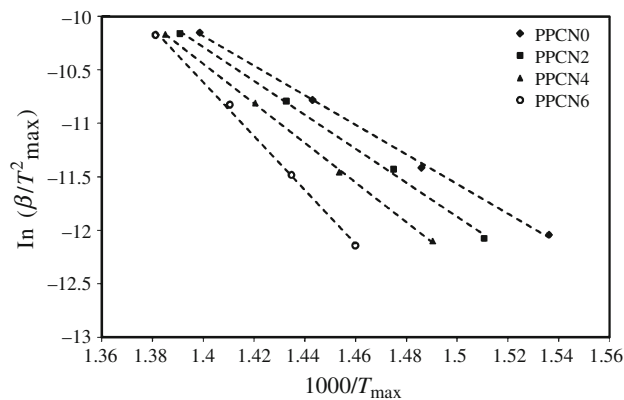
Kissinger assumed that the product  $n(1 - \alpha)_{max}^{n-1} = 1$  and it is independent of the heating rate. In such a case, the logarithmic expression of Eq. 8 can be written as

$$\ln \frac{\beta}{T_{max}^2} = -\frac{E_a}{R} \left( \frac{1}{T_{max}} \right) + \ln \frac{AR}{E}. \quad (9)$$

Thus, the activation energy can be computed from the linear relationship of the  $\ln(\beta/T_{max}^2)$  versus  $1/T_{max}$  plot for various heating rates.

Figure 3 shows the plots based on the Kissinger method, and the slopes of the lines drawn through these plots equal  $\Delta E_a/R$ . Thus, the activation energy,  $\Delta E_a$ , is determined. The parameters used and the results of  $\Delta E_a$  are listed in Table 2.

Comparing the results in Tables 1 and 2, the activation energies determined by the Ozawa and the Kissinger methods are quite comparable. From both methods, the  $E_a$

**Fig. 3** Plots of  $\ln(\beta/T_{max}^2)$  against  $1000/T_{max}$  of PPCN0, PPCN2, PPCN4, and PPCN6 for the Kissinger method.  $\beta$  is the heating rate and  $T_{max}$  is the absolute temperature at which the maximum degradation occurs

value obtained for PP in the pure form is smaller than those for the composites, which suggests that PP in the pure form could decompose more easily than that in the composites. In other words, PP in the nanoclay composites required higher activation energy than that in the pure form for thermal decomposition. Thus, it can be concluded that in the presence of MMT nanoclay, the thermal stability of PP is greatly improved.

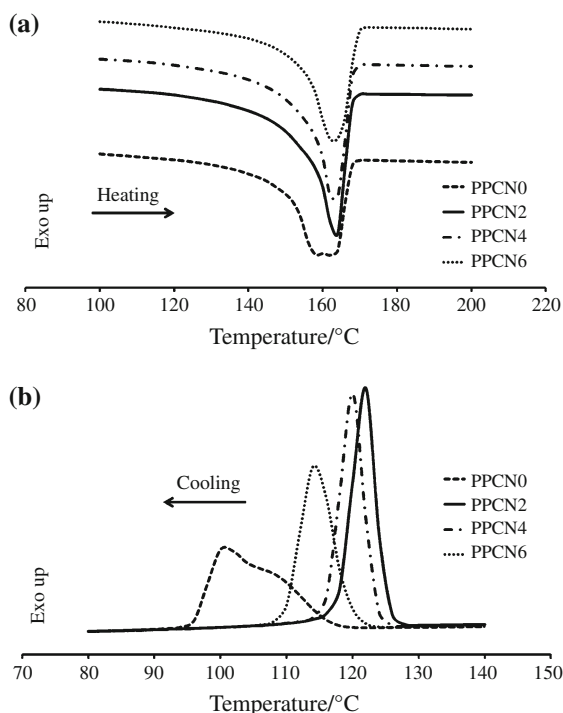
#### Non-isothermal melting and crystallization of MMT clay/MAH-PP nanocomposites

DSC melting thermographs of PPCNs are shown in Fig. 4a. From this figure, it is clearly seen that each sample, except for PPCN0, showed a single melting peak. But for the neat PP (PPCN0), an additional peak to the main melting one was observed. This double melting peak phenomenon of PPCN0 would be generally due to the polymorphism of PP. Labour et al. [26] reported that the melting temperatures of the  $\alpha$ - and the  $\beta$ -phase PP crystallites were around 165 and 150 °C, respectively. Therefore, the shoulder melting peak of PPCN0 at 149.7 °C, in Fig. 4a, should be attributed to  $\beta$ -form crystallites while the higher temperature one at 162.4 °C is due to the  $\alpha$ -form. To our surprise, this low temperature melting peak disappeared in the cases of PPCN2, PPCN4, and PPCN6 in which MMT nanoclay had been added. The results verified the inhibition effect of nanoclay on the formation of the  $\beta$ -phase crystallites.

Figure 4b shows the DSC cooling thermograms for PPCN0, PPCN2, PPCN4, and PPCN6. The crystallization curves show that the nanocomposites crystallized at higher temperatures (122.1, 120.0, and 114.5 °C for PPCN2, PPCN4, and PPCN6, respectively) with respect to the pure PP (105.2 °C), indicating that the addition of nanoclay

**Table 2** Thermal degradation kinetics parameters for PPCNs with different compositions and the activation energies for thermal degradation based on the Kissinger method

Sample code	$T_s/^\circ\text{C}$				$T_{\max}/^\circ\text{C}$				Activation energy/ $\text{kJ mol}^{-1}$
	Heating rate/ $^\circ\text{C min}^{-1}$				Heating rate/ $^\circ\text{C min}^{-1}$				
	2.5	5	10	20	2.5	5	10	20	
PPCN0	357	372	385	407	375	400	420	432	119.1
PPCN2	373	385	408	413	386	405	425	436	136.8
PPCN4	382	401	414	418	395	415	431	439	155.6
PPCN6	382	391	415	427	408	424	436	441	212.4

**Fig. 4** The DSC melting (a) and crystallization (b) curves of PPCN composites at the heating rate of  $10^\circ\text{C min}^{-1}$ 

particles effectively increased the crystallization temperature of PP. The biggest difference in crystallization was observed between the pure PP and PPCN2. The PPCN2 nanocomposite crystallized at a much higher temperature ( $122.1^\circ\text{C}$ ) than that ( $105.2^\circ\text{C}$ ) of pure PP. This large shifting in the non-isothermal crystallization temperature of PP indicates that the crystallization was facilitated in the presence of MMT clay. It is considered that MMT nanoclay played as a nucleating agent and as a result, crystallization of PP was accelerated. Unfortunately, it is also found that the addition of an excessive amount of nanoclay in PP would gradually reduce the crystallization temperatures as in the cases of PPCN4 and PPCN6. The sharp peaks of crystallization observed for PPCN2 and PPCN4 would mean the formation of a single form and more perfect crystals.

### Crystallinity of PP in the presence of MMT clay

As the heat absorbed in a melting process is only concerned with the crystalline portion of a material, a perfect crystalline material will absorb the maximum heat in its melting process. However, in the case of a semicrystalline material, where the whole volume of the material is not fully crystalline and there is more or less portion of amorphous structure. The heat of fusion of the semicrystalline material depends on the fraction of crystalline region. Therefore, the crystallinity of a sample ( $\chi_c$ ) can be determined by the following equation:

$$\chi_c = \frac{\Delta H_f}{\Delta H_f^0(1 - m_t)}, \quad (10)$$

where,  $\Delta H_f$  is the heat of fusion during melting,  $\Delta H_f^0$  is the theoretical specific melting heat of 100% crystalline isotactic PP, which is taken as  $165 \text{ J g}^{-1}$  [27], and  $m_t$  is the mass fraction of the filler. By using this value of  $\Delta H_f^0$ , the crystallinities of PPCNs are obtained in Table 3.

It could be seen from Table 3 that the composite materials have higher crystallinities than pure PP. But for PPCN4 and PPCN6, they have less crystallinities than PPCN2. This is because the addition of an excess amount of nanoclay fillers would reduce the chain mobility of the polymer and then prevent the polymer from formation of crystalline structure. Therefore, PPCN4 and PPCN6 have the lower crystallinities than PPCN2. This phenomenon is also in agreement with our previous work on CNT/PP composites [2]. From this result, we can draw a conclusion that the addition of certain amount of nanoclay filler helps to improve crystallinity of PP. This phenomenon can also be explained by means of the activation energy required for the crystallization as discussed further in the following section.

### Non-isothermal crystallization kinetics of MMT clay/MAH-PP nanocomposites

The crystallization temperature of a polymer varies with the cooling rate applied during solidification. Therefore,

**Table 3** Melting behavior of PPCN composites at different heating rates where  $\Delta H_f$  is the heat of diffusion,  $T_m$  is the melting peak temperatures, and  $X_c$  is the crystallinity

Sample code	$T_m/^\circ\text{C}$				$\Delta H_f/\text{J g}^{-1}$				$\chi_c/\%$			
	Heating rate/ $^\circ\text{C min}^{-1}$				Heating rate/ $^\circ\text{C min}^{-1}$				Heating rate/ $^\circ\text{C min}^{-1}$			
	2.5	5	10	20	2.5	5	10	20	2.5	5	10	20
PPCN0	165	163	162	162	85.5	84.0	78.7	75.7	51.8	50.1	47.7	45.9
PPCN2	167	164	164	164	96.8	95.5	93.0	87.8	58.7	57.9	56.4	53.2
PPCN4	169	163	163	163	95.0	94.7	89.1	86.3	57.5	57.4	54.0	52.3
PPCN6	169	163	163	162	88.8	86.4	81.0	80.2	53.8	52.4	49.1	48.6

the Kissinger method [22] can also be applied for calculation of activation energy of crystallization. From Eq. 9, we can clarify that the crystallization of a polymer is affected by two parameters: one is the dynamic factor, which depends on the cooling rate, and the other is the static factor needed to overcome the energy barrier for the formation of crystal, which depends on the characteristic

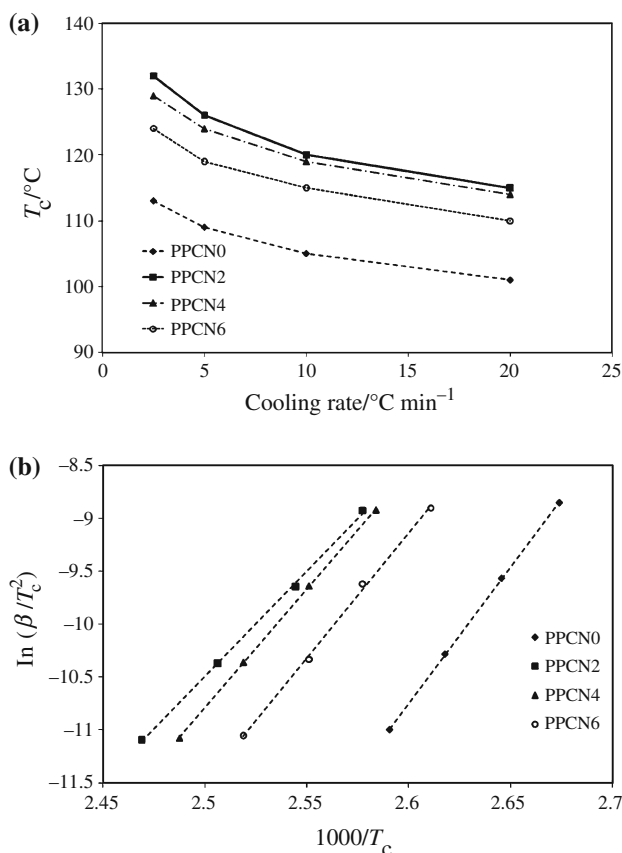
property of a material. The former is related to the activation energy for the transportation of molecular chains into crystals while the latter is related to the free energy barrier for the nucleation [28].

Figure 5a shows the variation of the crystallization temperature ( $T_c$ ) with the cooling rate ( $\beta$ ) applied. Therefore, the variation of the peak crystallization temperatures ( $T_c$ ) with respect to the cooling rate ( $\beta$ ) can be used to calculate the activation energy required in a non-isothermal crystallization process. To evaluate the activation energy of crystallization, Eq. 11 can be differentiated with respect to  $1/T_c$ . Then, this equation becomes:

$$\frac{d[\ln(\beta/T_c^2)]}{d(1/T_c)} = -\frac{\Delta E_a}{R} \tag{11}$$

where,  $T_c$ ,  $R$ , and  $\beta$  are the crystallization peak temperature, the universal gas constant, and cooling rate, respectively.

Figure 5b represents the plots based on the Kissinger method. From slopes of the fitted lines drawn across the points on the plots, the activation energies ( $\Delta E_a$ ) of PPCN composites were estimated and listed in Table 4. Knowing from this table, the values of  $\Delta E_a$  for the composites were smaller than that of pure PP. It is well known that the smaller the activation of crystallization, the easier the sample forms into a crystal structure. Therefore, the lower



**Fig. 5** a Crystallization peak temperature ( $T_c$ ) against cooling rate ( $\beta$ ) for PPCN composites and b Plots of  $\ln(\beta/T_c^2)$  against  $1000/T_c$  of PPCN0, PPCN2, PPCN4, and PPCN6 for the Kissinger method.  $\beta$  is the cooling rate and  $T_c$  is the absolute temperature at which the maximum crystallization occurs

**Table 4** Crystallization behavior of PPCN composites at different cooling rates where  $T_c$  is the crystallization peak temperatures and the activation energies were calculated using the Kissinger method

Sample code	$T_c/^\circ\text{C}$				Activation energy/ $\text{kJ mol}^{-1}$
	Cooling rate/ $^\circ\text{C min}^{-1}$				
	2.5	5	10	20	
PPCN0	112	110	105	99	212.8
PPCN2	131	125	122	119	167.2
PPCN4	128	123	120	117	184.7
PPCN6	123	118	114	110	198.5

activation energy of crystallization of PPCN2 allowed itself to form crystal easily and as a result it had a higher crystallinity than the rest. However, the  $\Delta E_a$  increased gradually with increase in the MMT nanoclay content. These increases in the activation energies made PPCN4 and PPCN6 to have lower crystallinities than PPCN2. This result agrees with one reported in the crystallinity section previously that an excess amount of nanoclay fillers would prevent the formation of crystalline structure by reducing chain mobility of the polymer.

## Conclusions

The thermal kinetics of montmorillonite nanoclay (MMT)/maleic anhydride-modified polypropylene (MAH-PP) nanocomposites were studied by means of thermal stability, melting and crystallization measurements, and theoretical analyses. The activation energies of thermal degradation of MMT/MAH-PP composites have been evaluated by both the Ozawa and the Kissinger methods. The activation energies of thermal degradation obtained by the Ozawa method were quite analogous with those by the Kissinger method. Both methods confirmed that the presence of MMT nanoclay improved the thermal stability of PP due to the enhanced activation energy of degradation. This higher activation energy of degradation made the composites more thermally stable. The study on the crystallization kinetics showed that the addition of 2 mass% of MMT nanoclay into PP enhanced its crystallinity but an excess amount of MMT could prevent the formation of crystals in the composites. According to the Kissinger method on crystallization, the declination in the activation energy resulted in improvement in the crystallinity of MMT/MAH-PP composites. Finally, it was verified that MMT nanoclay served as a nucleating agent during the non-isothermal crystallization and as a result the crystallinity of PP in the nanocomposites was significantly enhanced.

## References

- Ajayan PM, Schadler LS, Braun PV. Nanocomposite science and technology. Weinheim: Wiley-VCH; 2003.
- Sahoo NG, Thet NT, Tan QH, Li L, Chan SH, Zhao J, Yu S. Effect of carbon nanotubes and processing methods on the properties of carbon nanotube/polypropylene composites. *J Nanosci Nanotechnol*. 2009;9:5910–9.
- Sahoo NG, Rana S, Cho JW, Li L, Chan SH. Polymer nanocomposites based on functionalized carbon nanotubes. *Prog Polym Sci*. 2010;35:837–67.
- Cheng HKF, Sahoo NG, Pan Y, Li L, Chan SH, Zhao J, Chen G. Complementary effects of multi-walled carbon nanotubes and conductive carbon black on polyamide 6. *J Polym Sci Polym Phys*. 2010;48:1203–12.
- Zheng W, Lu XH, Toh CL, Zheng TH, He C. Effects of clay on polymorphism of polypropylene/clay nanocomposites. *J Polym Sci Polym Phys*. 2004;42:1810–6.
- Hambir S, Bulakh N, Jog JP. Polypropylene/Clay nanocomposites: effect of compatibilizer on the thermal, crystallization and dynamic mechanical behavior. *Polym Eng Sci*. 2002;42:1800–7.
- Maiti P, Nam PH, Okamoto M, Kotaka T, Hasegawa N, Usuki A. The effect of crystallization on the structure and morphology of polypropylene/clay nanocomposites. *Polym Eng Sci*. 2002;42:1864–71.
- Kato M, Okamoto H, Hasegawa N, Tsukigase A, Usuki A. Preparation and properties of polyethylene-clay hybrids. *Polym Eng Sci*. 2003;43:1312–6.
- Xu WB, Ge ML, He PS. Non-isothermal crystallization kinetics of polypropylene/montmorillonite nanocomposites. *J Polym Sci Polym Phys*. 2002;40:408–14.
- Maiti P, Nam PH, Okamoto M, Hasegawa N, Usuki A. Influence of crystallization on intercalation, morphology, and mechanical properties of polypropylene/clay nanocomposites. *Macromolecules*. 2002;35:2042–9.
- Qian G, Cho JW, Lan T. Polyolefin nanocomposites; Technical Papers; Nanocor, Inc. 2008. [http://www.nanocor.com/tech\\_papers/properties\\_polyolefin.asp](http://www.nanocor.com/tech_papers/properties_polyolefin.asp).
- Practical notes for TA DSC 2920. New Castle: TA Instruments Inc. 1990. <http://www1.chm.colostate.edu/Files/CIFDSC/dsc2000.pdf>.
- Ehrenstein GW, Riedel G, Trawiel P. Thermal analysis of plastics, theory and practices. Munich: Hanser Publishers; 2005.
- Practical notes for Hi-Res<sup>®</sup> TGA-2950. New Castle: TA Instruments Inc. 1990. <http://www1.chm.colostate.edu/Files/CIFDSC/TGA-MS.pdf>.
- TA-023. Thermal applications notes. TA Instruments Thermal Analysis and Rheology 1990. [http://www.tainstruments.co.jp/application/pdf/Thermal\\_Library/Applications\\_Briefs/TA023.PDF](http://www.tainstruments.co.jp/application/pdf/Thermal_Library/Applications_Briefs/TA023.PDF).
- Bernhard W. Thermal analysis of polymeric materials. Berlin: Springer; 2005.
- Sahoo NG, Cheng HKF, Cai J, Li L, Chan SH, Zhao J, Yu S. Improvement of mechanical and thermal properties of carbon nanotube composites through nanotube functionalization and processing methods. *Mater Chem Phys*. 2009;117:313–20.
- Sahoo NG, Cheng HKF, Li L, Chan SH, Judeh Z, Zhao J. Specific functionalization of carbon nanotubes for advanced polymer nanocomposites. *Adv Funct Mater*. 2009;19:3962–71.
- Sahoo NG, Cheng HKF, Pan Y, Li L, Chan SH, Zhao J. Strengthening of liquid crystalline polymer by functionalized carbon nanotubes through interfacial interaction and homogeneous dispersion. *Polym Adv Technol*. 2010. doi: 10.1002/pat.1704.
- Cheng HKF, Sahoo NG, Khin TH, Li L, Chan SH, Zhao J, Juay YK. The role of functionalized carbon nanotubes in a PA6/LCP blend. *J Nanosci Nanotechnol*. 2010;10:5242–51.
- Pramoda KP, Chung TS, Lui SL, Oikawa H, Yamaguchi A. Characterization and thermal degradation of polyimide and polyimide liquid crystalline polymers. *Polym Degrad Stabil*. 2000;67:365–74.
- Kissinger HE. Variation of peak temperature with heating rate in differential thermal analysis. *J Res Natl Bur Stand*. 1956;57:217–21.
- TA-125. Thermal applications notes. TA Instruments Thermal Analysis and Rheology 1990. [http://www.tainstruments.co.jp/application/pdf/Thermal\\_Library/Applications\\_Briefs/TA125.PDF](http://www.tainstruments.co.jp/application/pdf/Thermal_Library/Applications_Briefs/TA125.PDF).
- TA-075. Thermal applications notes. TA Instruments Thermal Analysis and Rheology 1990. [http://www.tainstruments.com/library\\_download.aspx?file=TA075.PDF](http://www.tainstruments.com/library_download.aspx?file=TA075.PDF).



25. TA-090. Thermal applications notes. TA Instruments Thermal Analysis and Rheology 1990. [http://www.tainstruments.co.jp/application/pdf/Thermal\\_Library/Applications\\_Briefs/TA090.PDF](http://www.tainstruments.co.jp/application/pdf/Thermal_Library/Applications_Briefs/TA090.PDF).
26. Labour T, Gauthier C, Seguela R, Vigier G, Bomal Y, Orange G. Influence of the  $\beta$  crystalline phase on the mechanical properties of unfilled and  $\text{CaCO}_3$ -filled polypropylene I. Structural and mechanical characterization. *Polymer*. 2001;42:7127–35.
27. Howe DV. In: Mark JE, editor. *Polymer data handbook*. London: Oxford University Press; 1999. p. 780–786.
28. Yuan Q, Awate S, Misra RDK. Nonisothermal crystallization behavior of polypropylene–clay nanocomposites. *Eur Polym J*. 2006;42:1994–2003.